Diagnostic performance of a whole-body dynamic ⁶⁸GA-DOTATOC PET/CT acquisition to differentiate physiological uptake of pancreatic uncinate process from pancreatic neuroendocrine tumor

Philippe Thuillier, MD[a,b,*], David Bourhis, MSc[b,c] [iD], Nicolas Karakatsanis, PhD[d] [iD], Ulrike Schick, MD, PhD[e], Jean Philippe Metges, MD, PhD[f], Pierre-Yves Salaun, MD, PhD[b,c] [iD], Véronique Kerlan, MD, PhD[a,b], Ronan Abgral, MD, PhD[b,c]

Abstract

To evaluate the diagnostic performance of net influx rate (Ki) values from a whole-body dynamic (WBD) ⁶⁸Ga-DOTATOC-PET/CT acquisition to differentiate pancreatic neuroendocrine tumors (pNETs) from physiological uptake of pancreatic uncinate process (UP).

Patients who were benefited from a WBD acquisition for the assessment of a known well-differentiated neuroendocrine tumor (NET)/suspicion of disease in the prospective GAPET-NET cohort were screened. Only patients with a confirmed pNET/UP as our gold standard were included. The positron emission tomography (PET) procedure consisted in a single-bed dynamic acquisition centered on the heart, followed by a whole-body dynamic acquisition and then a static acquisition. Dynamic (Ki calculated according to Patlak method), static (SUVmax, SUVmean, SUVpeak) parameters, and tumor-to-liver and tumor-to-spleen ratio (TLRKi and TSRKi (according to hepatic/splenic Ki)), tumor SUVmax to liver SUVmax (TM/LM), tumor SUVmax to liver SUVmean (TM/Lm), tumor SUVmax to spleen SUVmax (TM/SM), and tumor SUVmax to spleen SUVmean (TM/Sm) (according to hepatic/splenic SUVmax and SUVmean respectively) were calculated. A Receiver Operating Characteristic (ROC) analysis was performed to evaluate their diagnostic performance to distinguish UP from pNET.

One hundred five patients benefited from a WBD between July 2018 and July 2019. Eighteen (17.1%) had an UP and 26 (24.8%) a pNET. For parameters alone, the Ki and SUVpeak had the best sensitivity (88.5%) while the Ki, SUVmax, and SUVmean had the best specificity (94.4%). The best diagnostic accuracy was obtained with Ki (90.9%). For ratios, the TLRKi and the TSRKi had the best sensitivity (95.7%) while the TM/SM and TM/Sm the best specificity (100%). TLRKi had the best diagnostic accuracy (95.1%) and the best area under the curve (AUC) (0.990).

Our study is the first one to evaluate the interest of a WBD acquisition to differentiate UP from pNETs and shows excellent diagnostic performances of the Ki approach.

Abbreviations: AUC = area under the curve, CT = computerized tomography, IU = indeterminate uptake, Ki = net influx rate, MRI = magnetic resonance imaging, MTV = metabolic tumor volume, NET = neuroendocrine tumor, PET = positron emission tomography, PET/CT = positron emission tomography/computerized tomography, PET/MRI = positron emission tomography/magnetic resonance imaging, pNET = pancreatic neuroendocrine tumor, ROC = Receiver Operating Characteristic, SUV = standardized uptake value, TLG = total lesion glycolysis, TLR = tumor-to-liver ratio, TSR = tumor-to-spleen ratio, TM/LM = tumor SUVmax to liver SUVmax, TM/Lm = tumor SUVmax to liver SUVmean, TM/SM = tumor SUVmax to spleen SUVmax, TM/Sm = tumor SUVmax to spleen SUVmean, UP = pancreatic uncinate process, VOI = volume of interest, WBD = whole-body dynamic.

---

1. Introduction

^{68}Ga-DOTApeptides positron emission tomography coupled to computed tomography (PET/CT) has significantly contributed to improve diagnosis, staging, and monitoring of patients with neuroendocrine tumors (NETs) including pancreatic primary location. The high uptake of ^{68}Ga-DOTApeptides into pancreatic NETs has been extensively described in the literature, and the mean SUVmax in these tumors is usually higher than the NETs from other primary localization[1–3] with however a very wide range of standardized uptake values (SUVs) according to the series.

Physiological pancreatic uptake, especially in the head and in pancreatic uncinate process, has been reported as a frequent uptake in ^{68}Ga-DOTApeptides PET/CT. The hypotheses to explain this pancreatic uncinate uptake (UP) is a predominance of endocrine cells islets and/or a cellular hyperplasia expressing somatostatin receptor (SST).[4,5] This physiological activity can sometimes be difficult to distinguish from pancreatic tumors, proximal midgut tumors, or peritoneal nodular metastases, and requires careful evaluation of computed tomography (CT) or magnetic resonance imaging (MRI) images to confirm the absence of associated morphological abnormalities. It is therefore a classic pitfall that can lead to misdiagnose a pancreatic tumor.[5,6]

The differential diagnosis between pancreatic neuroendocrine tumor (pNET) and UP is therefore important. This topic has already been explored in the literature. In ^{68}Ga-DOTApeptides PET/CT, the SUVmax of the pNETs seems higher in comparison to the SUVmax of the UP, although there is a certain overlap of the values.[6–9] Prasad et al have suggested a SUVmax cut-off of 8.6 in their cohort to make the differential diagnosis between UP/ pNET.[6] However, another study enrolling 96 patients, failed to find a SUVmax threshold allowing obtaining good diagnostic sensitivity and specificity.[7] Finally, a recent study investigated the value of a PET/MRI acquisition in a single combined system, allowing an optimal co-localization of abnormalities detected with both modalities. The authors concluded that the presence of a diffuse uptake with a low SUVmax value associated with the absence of abnormality in diffusion-weighted images allowed to improve interpretive confidence.[9]

Recently multi-step or flow motion acquisition protocols have been developed and are achievable on new generation digital positron emission tomography (PET) machines, allowing to perform a 4D whole-body dynamic acquisition.[10–12] Dynamic PET/CT acquisitions allow to assess the net influx rate (Ki) of a lesion and this approach has already been used in whole-body dynamic (WBD) [18]FDG-PET/CT to differentiate malignant/ benign and pathological/physiological processes.[10] The hypothesis of our study is that Ki could be more discriminating than SUV approach to differentiate NETs from UP in ^{68}Ga-DOTATOC-PET/CT imaging.

The objective was to evaluate the diagnostic performance of Ki approach resulting from a dynamic whole-body acquisition in ^{68}Ga-DOTATOC-PET/CT to differentiate the pNET from the UP.

2. Materials and methods

This is a prospective monocentric ancillary study of the GAPET-NET study (NCT03576040).

2.1. Population

The inclusion criteria were as follows: patient having an indication to a ^{68}Ga-DOTATOC-PET/CT for the assessment of a well-differentiated neuroendocrine tumor (NET) or suspicion of disease, benefited from a whole-body dynamic ^{68}Ga-DOTATOC-PET/CT acquisition and for whom a lesion suggestive of pancreatic NET localization (primary pancreatic NET or metastasis of a NET from another known primary localization) or a fortuitous UP were discovered. Criteria for non-inclusion were: history of total pancreatectomy excluding the possibility of NET pancreatic localization or UP; no abnormal uptake on pancreas visualized; abnormal uptake whose the pancreatic origin remain uncertain on morphological finding on the CT (in particular doubt about peripancreatic lymph node).

The protocol was approved by the medical ethics committee (29BRC17.0036) and all included patients expressed their non-opposition to achieving the dynamic acquisition and participation of this study.

2.2. UP and NET definition

Regarding the comparison of the 2 populations, each lesion was classified as UP, pNET, or indeterminate uptake (IU) according to the following gold standard. Pathological uptakes classified as pNET were those corresponding to a focal uptake with morphological findings confirmed on the enhanced CT coupled to PET and/or other imaging and/or histological confirmation. Physiological uptakes classified as UP were those with a diffuse uptake aspect of the uncinate process without morphological findings on the enhanced CT coupled to PET and/or other imaging. If no NET was previously known in the patient, the absence of morphological findings had only to be confirmed on the enhanced CT coupled to PET. If a NET was already known (pNET or NET from another primary localization), the absence of morphological findings had to be confirmed on the enhanced CT coupled to PET and also on at least one other morphological imaging (abdominal MRI and or endoscopic ultrasonography).

Uptakes classified as IU were those with a diffuse uptake aspect of the uncinate process but with a doubtful morphological aspect or those with a focal uptake aspect without morphological findings.

2.3. Images acquisition and reconstruction

The ^{68}Ga-DOTATOC-PET/CT images were acquired on a latest-generation digital PET machine (Biograph Vision; Siemens©, Erlangen, Germany). The acquisition was performed after the injection of approximately 2 MBq/kg of 68Ga-DOTATOC eluted with a Galliapharm generator (Eckert and Ziegler©, Berlin, Germany).

CT was obtained first in the craniocaudal direction using a whole-body protocol, after injection of intravenous iodine contrast agent (1.5 mL/kg), unless contraindicated. CT consisted of a 64-slice multidetector-row spiral scanner with the following standard parameters: tube voltage of 120 kV, and effective tube current of 80 mAs, 700 mm transverse field of view, 16 mm × 1.2 mm collimation, pitch 1.

The PET images were acquired in the craniocaudal direction and were reconstructed without and with attenuation correction using an iterative reconstruction algorithm (OSEM 3D) with time of fight correction and point spread function (Siemens© TrueXTM). The images were corrected for random coincidences, dispersion, and attenuation using CT data. The PET images were smoothed using a Gaussian filter (2 mm full-width at half-maximum). The size of the transaxial reconstruction matrix was 440 × 440 voxels and the voxel size was 1.65 mm × 1.65 mm × 1.65 mm.

Whole-body dynamic acquisition was performed using integrated workflow according to a methodology previously described by Karakatsanis et al.[10] The acquisition included a first 6-minutes single-bed acquisition (12 × 5 s, 6 × 10 s, 8 × 30 s) over the heart to acquire the initial part of the input function followed by a 60-minutes whole-body dynamic acquisition including 10 passes of 6 minutes/pass. The scanning speed was 4 mm s^{-1}.

All physiological volume of interest (VOI) and UP/pNET segmentation were performed with Syngovia software by a single nuclear medicine physician

2.4. Images derived input function

The total radioactivity concentration in the arterial plasma was used as an input function as previously described[11] and was generated from a VOI of 1 cm drawn over the left ventricle[12] in each image of the acquisition. The VOI was then projected on whole-body dynamic acquisition to generate the input function. Theoretically, an arterial blood sample is required to obtain the input function, but several studies have shown that the input function can be estimated only from image data.[13–15]

2.5. Time–activity and Patlak's graphical analysis

Time–activity curves were determined for VOI physiological uptake (liver, spleen) on whole-body dynamic acquisition. A VOI of 5 cm, placed on the right hepatic lobe and a VOI of at least 1 cm, placed on the spleen were used to obtain hepatic and splenic time-activity curves respectively. Time–activity curves were determined for pTNE or UP VOI identified and segmented based on a threshold of 40% of the voxel with the highest activity.

Net influx rate (Ki) (expressed in mL/min/100 mL) based on Patlak's graphical analysis was calculated for each VOI (Supplemental Figure, http://links.lww.com/MD/E266). Patlak's plots were generated according to the equation for each VOI from the parameters obtained from the 3rd to the 7th scans of the whole-body dynamic acquisition for each patient (18–48 minutes). Ki was calculated by linear regression of the following equation:

$$\frac{C_{DOTATOC}(t)}{C_p(t)} = Ki \frac{\int_0^t C_p(t)dt}{C_p(t)} + V_p$$

V_p: volume fraction of plasma in the VOI; C_p: arterial plasma blood concentration; and $C_{DOTATOC}$: tissue concentration.

2.6. Static images and SUV parameters calculation

Static images were generated from the last 2 scans (9th and 10th passes). Physiological (liver/spleen) and pTNE/UP VOIs of WBD acquisition were copied and used for static acquisition. Static PET metabolic parameters (SUVmax, SUVmean, SUV peak, metabolic tumor volume (MTV), and total lesion glycolysis (TLG = SUVmean × MTV) were calculated.

2.7. Tumor to liver and tumor to spleen ratio

Tumor-to-liver and tumor-to-spleen ratio were calculated for dynamic PET parameters (tumor-to-liver ratio (TLR) Ki and tumor-to-spleen ratio (TSR) Ki according to hepatic and splenic Ki) and statics PET parameters (tumor SUVmax to liver SUVmax (TM/LM), tumor SUVmax to liver SUVmean (TM/Lm), tumor SUVmax to spleen SUVmax (TM/SM) and tumor SUVmax to spleen SUVmean (TM/Sm) according to hepatic and splenic SUVmax and SUVmean respectively).

3. Statistical analysis

Receiver Operating Characteristic (ROC) analysis was used to assess the diagnostic performance of each variable (to differentiate between pNET and UP). Youden index was used to find each variable's best cut-off point.[16] Area under the curves (AUC), sensitivity, specificity, and accuracy were reported.

Significance level of P-value was .05. All statistical analyses were performed using XLSTAT life software (Addinsoft©, Paris, France).

4. Results

One hundred five patients benefited from a whole-body dynamic acquisition between July 2018 and July 2019 were screened (age = 60.18 ± 15.35 years, sex ratio 55M/50F (52.4%/47.6%), weight 75.39 ± 15.88 kg with a static acquisition performed 53.3 ± 5.6 min after the injection of 2.63 ± 0.35 MBq/kg.

The selection of the population is described in the flowchart (Fig. 1). Six patients were excluded because of a history of total pancreatectomy (n = 3) or in case of lesion of uncertain pancreatic origin (n = 3). Fifty patients (47.6%) had neither UP nor NET. Of the 105 patients, 27 (25.7%) had a UP and 28 (26.6%) had a NET.

The comparison of the values of each parameter is shown in Table 1. All static and dynamic parameters were statistically higher in the pNET than in the UP group (P < .001). The volumetric parameters (MTV40% and TLG) were not discriminating. All TLR and TSR ratios were statistically higher in the NET compared to the UP (P < .0001). Regardless of the ratio used, no UP had superior value than physiological splenic uptake.

The diagnostic performance of each parameter is shown in Table 2. Considering the static and dynamic parameters, Ki and SUVpeak had the best sensitivity (88.5%) while Ki, SUVmax, and SUVmean had the best specificity (94.4%). Finally, the best diagnostic accuracy was obtained with Ki (90.9%). Considering TLR and TSR ratios, TLR Ki and TSR Ki had the highest sensitivity (95.7%) while TM/SM and TM/Sm had the best specificity (100%). Finally, the TLR Ki had the best diagnostic accuracy (95.1%).

ROC curves with AUC of static and dynamic parameters and TLR TSR ratios are shown in Figures 2 and 3. For parameters alone, SUVmax and SUVmean had the best AUC (0.953). For the
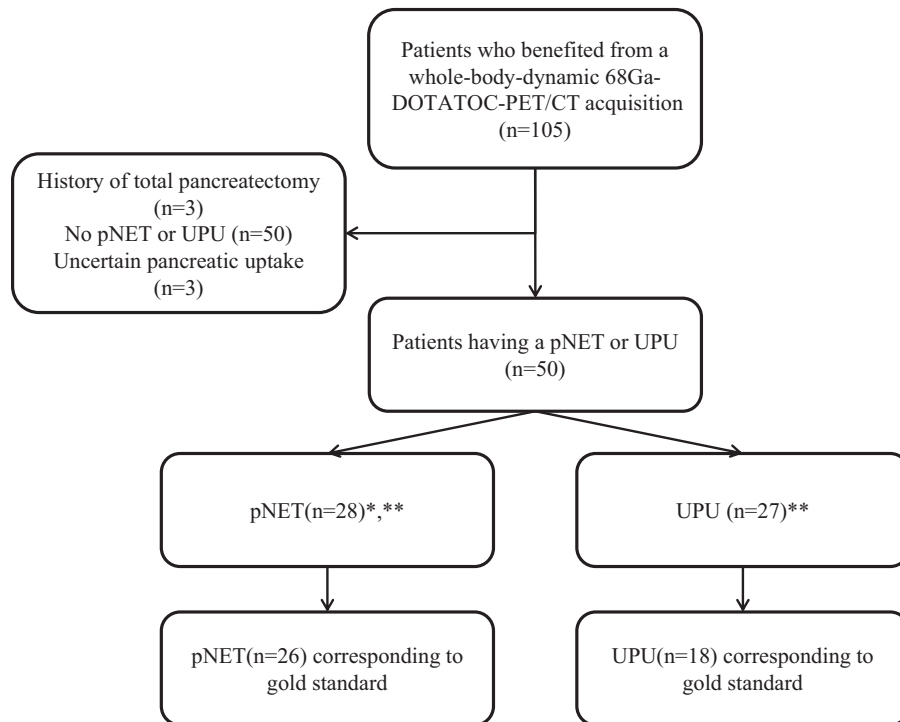
Figure 1. Flowchart selection of pNET and UP in our study. *2 lesions in 2 patients, **3 patients with a pNET and an UP.

TLR and TSR ratios, the TLR Ki had the best AUC (0.990). The performance of each parameter was not statistically different.

5. Discussion

Our study is the first study assessing the interest of a dynamic acquisition with Ki approach for the differential diagnosis between UP and TNE.

In [18]FDG-PET/CT, numerous studies have evaluated the interest of dynamic approach to differentiate benign and malignant pathologies for example in the context of the diagnosis of malignancy of a pulmonary tumor,[17] or in the context of post-therapeutic evaluation to distinguish post-therapeutic inflammatory reshaping and residual disease.[18] Therefore, we investigated the utility of this acquisition to differentiate the physiological UP from pNET in ^{68}Ga-DOTATOC-PET/CT imaging, which is a classic diagnostic pitfall.

Our results show excellent diagnostic performances of static and dynamic parameters, especially the TLR and TSR ratios and with the Ki approach. Regarding the prevalence of UP in our cohort, 25.7% of patients were concerned. These data are slightly lower than in the literature: 34.8% in the Graybriel et al study with ^{68}Ga-DOTATATE-PET/RMI,[9] 36.3% in the Krauz et al study with ^{68}Ga-DOTANOC-PET/CT[7] and 70% in the Jacobsson et al study with ^{68}Ga-DOTATOC-PET/CT.[8]

In SUV approach, our results show that static parameters have good performance with AUC of 0.93 for SUVmax and SUVmean, and 0.95 for SUVpeak. Our results are globally consistent with the data in the literature. In the Graybiel et al study in ^{68}Ga-DOTATATE-PET/MRI, the SUVmax values in the UP and pNET were globally comparable to those in our study (mean SUVmax of 10.5 ± 7.2 in UP versus median SUVmax of 13.62 in our cohort and mean SUVmax of 63.2 ± 52.0 in the pNET versus median SUVmax of 53.99 in our cohort). But the authors did not propose a cut-off.[9] Moreover, in the Prasad et al study, a SUV max cut-off of 8.6 obtained in ^{68}Ga-DOTANOC-PET/CT allowed having sensitivity and specificity of 92% and 94%, respectively.[6] With the same tracer, however, it was not found an optimal cut-off in Krauz et al study.[7] Finally, the study by Kroiss et al conducted in ^{68}Ga-DOTATOC-PET/CT found a cut-off of SUVmax=17.1 with sensitivity and specificity of 93.6% and 90.0%, respectively.[19]

In dynamic approach, the median Ki had comparable performances with an AUC of 0.93 but a diagnostic accuracy

Table 1

Comparison between statics and dynamics PET parameters in pNET and UP.

Parameters	UP (n = 18)	pNET (n = 26)	P value
Ki	5.22 (2.06–27.06)	25.33 (4.93–137.41)	<.001
TLR Ki	1.74 (0.68–5.69)	11.49 (3.23–37.04)	<.001
TSR Ki	0.34 (0.17–0.82)	2.43 (0.41–10.97)	<.001
SUVmax lesion	13.62 (7.29–39.62)	53.99 (14.53–184.31)	<.001
SUVpeak lesion	9.11 (4.68–24.25)	31.81 (7.25–147.76)	<.001
SUVmean lesion	7.59 (3.86–23.3)	31.82 (8.03–114.60)	<.001
MTV40% (mL)	5.23 (0.98–13.65)	2.3 (0.33–78.13)	.09
TLG (g)	44.38 (5.32–128.32)	63.33 (4.88–3720.52)	.22
TM/LM	1.56 (0.76–3.98)	7.47 (2.06–21.06)	<.001
TM/Lm	2.57 (1.35–7.13)	13.23 (3.52–39.42)	<.001
TM/SM	0.43 (0.28–0.71)	2.77 (0.54–10.83)	<.001
TM/Sm	0.54 (0.36–0.88)	3.53 (0.68–16.18)	<.001

Values expressed in median (min–max).
Ki: net influx rate; MTV: metabolic tumor volume; pNET: pancreatic neuroendocrine tumor; SUV: standardized uptake value; TLG: total lesion glycolysis; TM/LM: tumor SUVmax/liver SUVmax; TM/LM: tumor SUVmax to liver SUVmax; TM/Lm: tumor SUVmax to liver SUVmean; TM/SM: tumor SUVmax to spleen SUVmax; TM/Sm: tumor SUVmax to spleen SUVmean; UP: pancreatic uncinate process.

Table 2

Areas under the curve (AUC), AUC 95% confidence intervals (CI), and diagnostic performance of statics and dynamics PET parameters.

Parameters	AUC	CI95%	*P* value	Cut-off	Se (%)	Sp (%)	Acc (%)
Ki	0.93	0.89–0.98	<.001	8.89	88.5	94.4	90.9
TLR Ki	0.99	0.99–0.99	<.001	4.56	95.7	94.4	95.1
TSR Ki	0.98	0.98–0.98	<.001	0.649	95.7	94.1	95.0
SUVmax	0.95	0.95–0.95	<.001	28.0	84.6	94.4	88.6
SUVpeak	0.93	0.88–0.97	<.001	14.78	88.5	83.3	86.4
SUVmean	0.95	0.95–0.95	<.001	17.75	84.6	94.4	88.6
TM/LM	0.98	0.98–0.98	<.001	3.76	91.0	94.4	92.5
TM/Lm	0.99	0.99–0.99	<.001	5.72	95.5	94.4	95.0
TM/SM	0.97	0.97–0.97	<.001	0.975	91.3	100	95.0
TM/Sm	0.97	0.97–0.97	<.001	1.32	91.3	100	95.0

Values expressed in median (min–max).

Acc: accuracy; AUC: area under the curve; CI95%: confidence intervals at 95%; Ki: net influx rate; MTV: metabolic tumor volume; pNET: pancreatic neuroendocrine tumor; Se: sensibility; Sp: specificity; SUV: standardized uptake value; TLG: total lesion glycolysis; TM/LM: tumor SUVmax to liver SUVmax; TM/Lm: tumor SUVmax to liver SUVmean; TM/SM: tumor SUVmax to spleen SUVmax; TM/Sm: tumor SUVmax to spleen SUVmean; UP: pancreatic uncinate process.

slightly higher of 90.9% but without significant differences compared to the static parameters, with a cut-off value of 8.89 mL/min/100 mL. There is no comparability with other data in the literature.

The diagnostic performance of the TLR and TSR ratios has been rarely evaluated in the literature. Our results suggest slightly higher diagnostic performance in our cohort compared to SUV and Ki parameters alone. In addition, the TLR Ki ratio in our cohort had the best diagnostic performance (AUC = 0.990, sensibility = 95.7%, specificity = 94.4%, and accuracy = 95.1%). Nevertheless, the performances were not statistically different from the TLR and TSR ratios. In the Froeling et al study, the
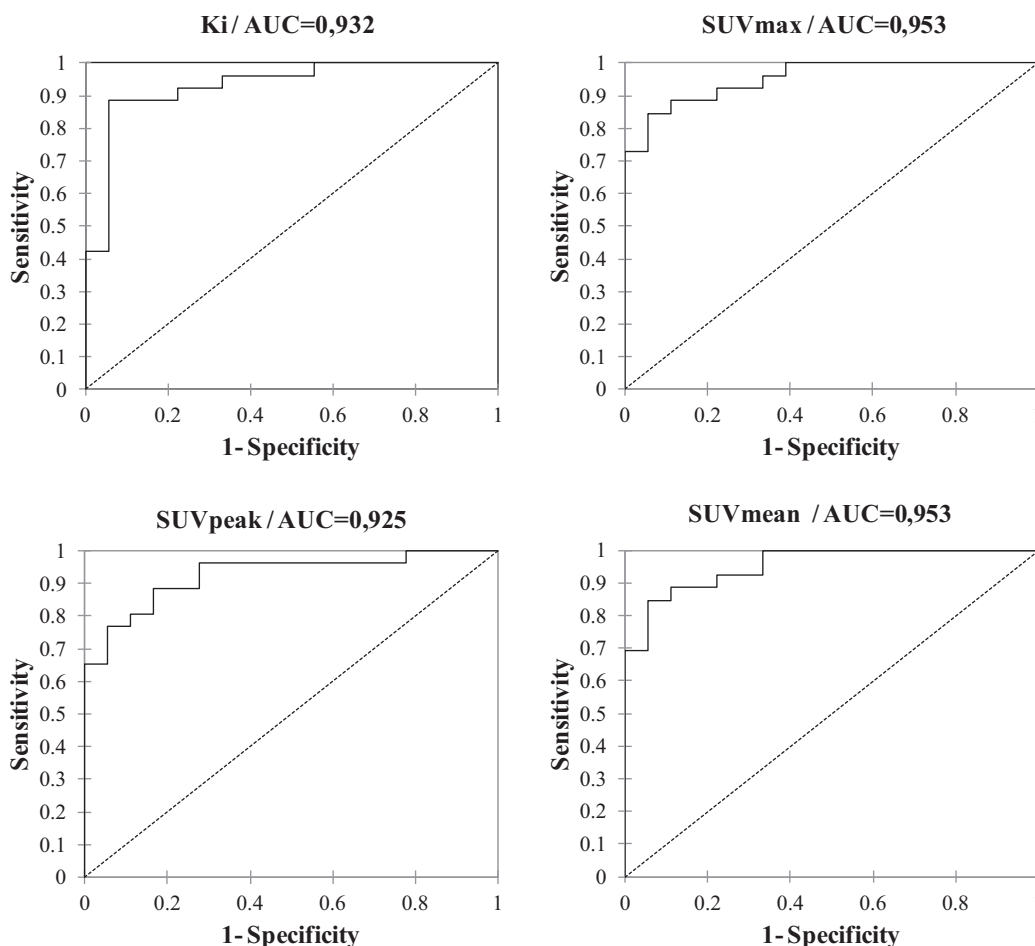

Figure 2. ROC curves with AUC using static and dynamic parameters alone to differentiate pNETs from UP.
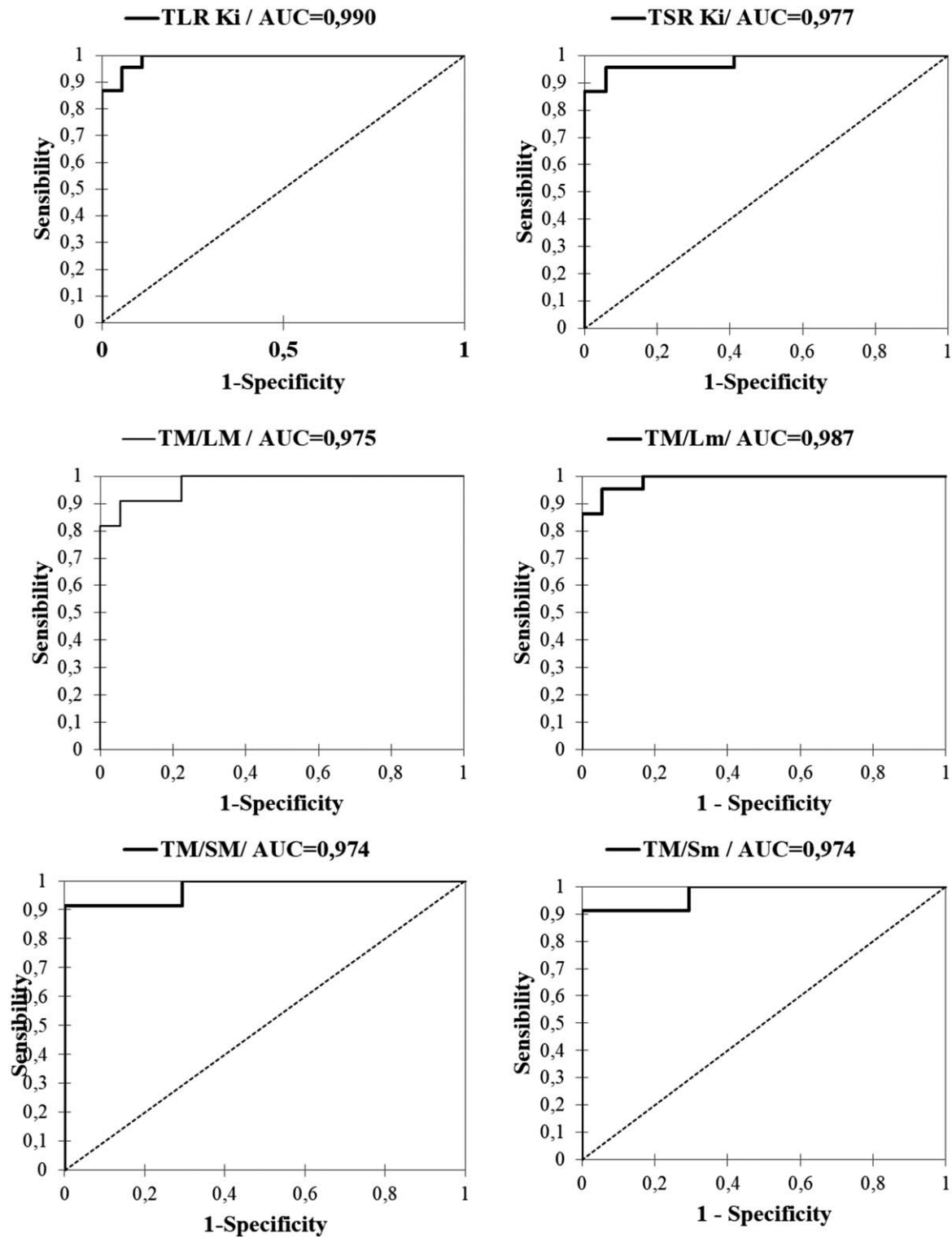
Figure 3. ROC curves with AUC using TLR and TSR ratios to differentiate pNETs from UP.

mean TLR of the NETs was 3.2 (min: 0.69, max: 23.1) versus 0.94 (min: 0.51, max: 1.5) in UP with a large overlap of values.[20] It should be noted that in our cohort, no UP had a superior uptake to the splenic SUV or splenic Ki that could make splenic uptake as a reference in visual and quantitative analyses to consider a pancreatic uptake as pathological.

One hypothesis could explain the very good performances of the different parameters of our study. Patients included in our cohort had an indication for a ^{68}Ga-DOTATOC-PET/CT for the evaluation of a well-differentiated NET with therefore expected elevated SUVmax values. If G3 NETs or neuroendocrine carcinoma had been included in our study, the performances

would probably have been lower due to the likely higher overlap of values between pNETs and UPs. In this point of view, development of PET/CT acquisition with a dual-tracer simultaneous administration of ^{18}FDG and ^{68}Ga-DOTApeptides to assess high G2/G3 NETs or neuroendocrine carcinoma would be useful and could allow differentiating non-^{68}Ga-DOTApeptides-avid NETs from Ups.[21]

The main limitations of our study are: a relatively small population; for ethic consideration, our gold standard does not use only histological data to confirm the diagnosis of pNET or UP.

Finally, it is important to note that our study is the first to evaluate whole-body dynamic and parametric ^{68}Ga-DOTA-TOCPET/CT acquisition in NETs. This technique has no impact on the patient in terms of radiation exposure. Although our results do not show a significant difference between the 2 approaches, our dynamic acquisition allows the measurement of Ki on all other regions of the body included in the acquisition protocol with perspectives in terms of diagnostic, prognostic or therapeutic evaluation in NETs. This would not be possible with dynamic single-bed acquisitions.[24] Furthermore, we are aware of the absence of a significant difference in performance between the SUV and Ki approaches in our study. However, the Ki approach will probably be more robust with more reproducible Ki values between different PET systems compared to the SUV approach which would allow defining more precise cut-off to differentiate UP from pNETs.

In conclusion, our study is the first study assessing the interest of a whole-body dynamic ^{68}Ga-DOTATOC-PET/CT acquisition to differentiate physiological uptake of the pancreatic uncinate process from pathological uptake. Our results suggest the excellent diagnostic performance of the Ki approach although its superiority over the standard SUV approach could not be established, even though the Ki approach contrast (TLR Ki) presented the best diagnostic accuracy. Further studies on a larger cohort including high-grade lesions are needed.

Author contributions

VK, PYS, RA are the guarantors of the paper.

PT, DB, NK, RA designed the study.

PT realized statistics.

PT drafted the manuscript.

PT, DB, RA did interpretation of data.

VK, PYS, RA, US, JPM, revised the manuscript for intellectual content.

All authors contributed in drawing up the manuscript.

References

[1] Campana D, Ambrosini V, Pezzilli R, et al. Standardized uptake values of 68Ga-DOTANOC PET: a promising prognostic tool in neuroendocrine tumors. J Nucl Med 2010;51:353–9.

[2] O'Toole D, Saveanu A, Couvelard A, et al. The analysis of quantitative expression of somatostatin and dopamine receptors in gastro-entero-pancreatic tumours opens new therapeutic strategies. Eur J Endocrinol 2006;155:849–57.

[3] Yu J, Li N, Li J, et al. The correlation between [68Ga]DOTATATE PET/CT and cell proliferation in patients with GEP-NENs. Mol Imaging Biol 2019;21:984–90.

[4] Virgolini I, Ambrosini V, Bomanji JB, et al. Procedure guidelines for PET/CT tumour imaging with 68Ga-DOTA-conjugated peptides: 68Ga-DOTA-TOC, 68Ga-DOTA-NOC, 68Ga-DOTA-TATE. Eur J Nucl Med Mol Imaging 2010;37:2004–10.

[5] Hofman MS, Lau WFE, Hicks RJ. Somatostatin receptor imaging with 68 Ga DOTATATE PET/CT: clinical utility, normal patterns, pearls, and pitfalls in interpretation. RadioGraphics 2015;35:500–16.

[6] Prasad V, Baum RP. Biodistribution of the Ga-68 labeled somatostatin analogue DOTA-NOC in patients with neuroendocrine tumors: characterization of uptake in normal organs and tumor lesions. Q J Nucl Med Mol Imaging 2010;54:61–7.

[7] Krausz Y, Rubinstein R, Appelbaum L, et al. Ga-68 DOTA-NOC uptake in the pancreas: pathological and physiological patterns. Clin Nucl Med 2012;37:57–62.

[8] Jacobsson H, Larsson P, Jonsson C, et al. Normal uptake of 68Ga-DOTA-TOC by the pancreas uncinate process mimicking malignancy at somatostatin receptor PET. Clin Nucl Med 2012;37:362–5.

[9] Graybiel CE, Hope T. Physiologic versus malignant uncinate process uptake on 68Ga-DOTA-TATE PET/MRI. J Nucl Med 2019;60:565–1565.

[10] Karakatsanis NA, Zhou Y, Lodge MA, et al. Generalized whole-body Patlak parametric imaging for enhanced quantification in clinical PET. Phys Med Biol 2015;60:8643–73.

[11] Karakatsanis NA, Lodge MA, Tahari AK, et al. Dynamic whole-body PET parametric imaging: I. Concept, acquisition protocol optimization and clinical application. Phys Med Biol. 2013;58:7391-7418. doi:10.1088/0031-9155/58/20/7391

[12] Karakatsanis NA, Lodge MA, Zhou Y, et al. Dynamic whole-body PET parametric imaging: II. Task-oriented statistical estimation. Phys Med Biol. 2013;58:7419-7445. doi:10.1088/0031-9155/58/20/7419

[13] Velikyan I, Sundin A, Sorensen J, et al. Quantitative and qualitative intrapatient comparison of 68Ga-DOTATOC and 68Ga-DOTATATE: net uptake rate for accurate quantification. J Nucl Med 2014;55:204–10.

[14] Chen K, Bandy D, Reiman E, et al. Noninvasive quantification of the cerebral metabolic rate for glucose using positron emission tomography, 18F-fluoro-2-deoxyglucose, the Patlak method, and an image-derived input function. J Cereb Blood Flow Metab 1998;18:716–23.

[15] Henze M, Schuhmacher J, Hipp P, et al. PET imaging of somatostatin receptors using [68GA]DOTA-D-Phe1-Tyr3-octreotide: first results in patients with meningiomas. J Nucl Med 2001;42:1053–6.

[16] Koukouraki S, Strauss LG, Georgoulias V, et al. Comparison of the pharmacokinetics of 68Ga-DOTATOC and [18F]FDG in patients with metastatic neuroendocrine tumours scheduled for 90Y-DOTATOC therapy. Eur J Nucl Med Mol Imaging 2006;33:1115–22.

[17] Van Binnebeek S, Koole M, Terwinghe C, et al. Dynamic 68Ga-DOTATOC PET/CT and static image in NET patients: correlation of parameters during PRRT. Nuklearmedizin 2016;55:104–14.

[18] Youden WJ. Index for rating diagnostic tests. Cancer 1950;3:32–5.

[19] Hübner KF, Buonocore E, Gould HR, et al. Differentiating benign from malignant lung lesions using 'quantitative' parameters of FDG PET images. Clin Nucl Med 1996;21:941–9.

[20] Choi H, Yoon H, Kim TS, et al. Voxel-based dual-time 18F-FDG parametric imaging for rectal cancer: differentiation of residual tumor from postchemoradiotherapy changes. Nucl Med Commun 2013;34:1166–73.

[21] Kroiss A, Putzer D, Decristoforo C, et al. 68Ga-DOTA-TOC uptake in neuroendocrine tumour and healthy tissue: differentiation of physiological uptake and pathological processes in PET/CT. Eur J Nucl Med Mol Imaging 2013;40:514–23.

[22] Froeling V, Röttgen R, Collettini F, et al. Detection of pancreatic neuroendocrine tumors (PNET) using semi-quantitative [68Ga]DOTA-TOC PET in combination with multiphase contrast-enhanced CT. Q J Nucl Med Mol Imaging 2014;58:310–8.

[23] Karakatsanis NA, Abgral R, Trivieri MG, et al. Hybrid PET- and MR-driven attenuation correction for enhanced 18F-NaF and 18F-FDG quantification in cardiovascular PET/MR imaging. J Nucl Cardiol 2019; published online Oct 30.

[24] Zaidi H, Karakatsanis N. Towards enhanced PET quantification in clinical oncology. BJR. 2017;91(1081):20170508. doi:10.1259/bjr.20170508